Skeletal Radiol (2011) 40:1355–1360
DOI 10.1007/s00256-011-1162-y

TECHNICAL REPORT

3T MR neurography using three-dimensional diffusion-weighted PSIF: technical issues and advantages

Avneesh Chhabra · Ty K. Subhawong · Cary Bizzell · Aaron Flammang · Theodoros Soldatos

Received: 30 January 2011 / Revised: 20 March 2011 / Accepted: 21 March 2011 / Published online: 15 April 2011

Abstract Three-dimensional (3D) diffusion-weighted reversed fast imaging with steady state precession (3D DW-PSIF) MR sequence has the potential to create nerve-specific images. The authors describe the technical issues and their initial experience with this imaging technique employed for peripheral MR neurography.

Keywords 3D DW-PSIF · MR neurography · Vascular suppression · Peripheral nerves

Introduction

Magnetic resonance imaging is being increasingly used for peripheral nerve evaluation. Similar signal intensity of nerves and vessels may make their discrimination difficult. The three-dimensional (3D) diffusion-weighted reversed fast imaging with steady state precession (3D DW-PSIF) sequence is a magnetic resonance (MR) imaging technique that has been used in the evaluation of the cranial nerves and lumbar plexus with good vascular suppression [1–7]. In assessing the value of 3D DW-PSIF for the evaluation of peripheral nerves, we address technical issues and describe our initial experience.

A. Chhabra (✉) · T. K. Subhawong · C. Bizzell · T. Soldatos
The Russell H. Morgan Department of Radiology and Radiological Science, The Johns Hopkins Hospital,
601 North Caroline Street, Room 4214,
Baltimore, MD 21287, USA
e-mail: achhabr6@jhmi.edu

A. Flammang
Siemens Medical Solutions, USA Inc,
Malvern, PA, USA

Technical issues

The 3D DW-PSIF belongs to the family of steady-state sequences. It is a balanced gradient echo steady-state free precession sequence encompassing inherent features of a spin-echo sequence with less influence of local magnetic field inhomogeneities on the spin relaxation [6]. Although 3D DW-PSIF may also be performed without fat saturation, fat-suppressed images usually provide better nerve to background contrast ratio in peripheral nerve imaging. In the authors' experience, the selective water-excitation type fat suppression technique enables most uniform fat suppression and is unaffected by the chemical shift effects. Due to the steady state nature and low diffusion moment, there is adequate suppression of the vascular signal on this sequence creating nerve selective images. In most cases, a diffusion moment value of 80–90 s mm^{-2} s^{-1} provides an acceptable compromise in peripheral nerve-to-background contrast and image signal-to-noise ratios (Fig. 1). As a result, the high T2 signal intensity of peripheral nerves is effectively differentiated from the nulled signal of adjacent vessels. The field of view should be generally limited to 10–15 cm to avoid ghosting artifacts and maintain enough signal to noise ratio (SNR) in the image (Fig. 2). Imaging is better accomplished on coronal or sagittal planes to keep the acquisition time low. With shimming, the overall additional time beyond the MR neurography protocol is close to 6 min. The imaging parameters on a 3 T Verio/Trio MR scanner (Siemens Medical Solutions, Erlangen, Germany) are outlined in Table 1.

Imaging evaluation

The 3D DW-PSIF sequence is an isotropic sequence with submillimeter resolution. Following evaluation of the

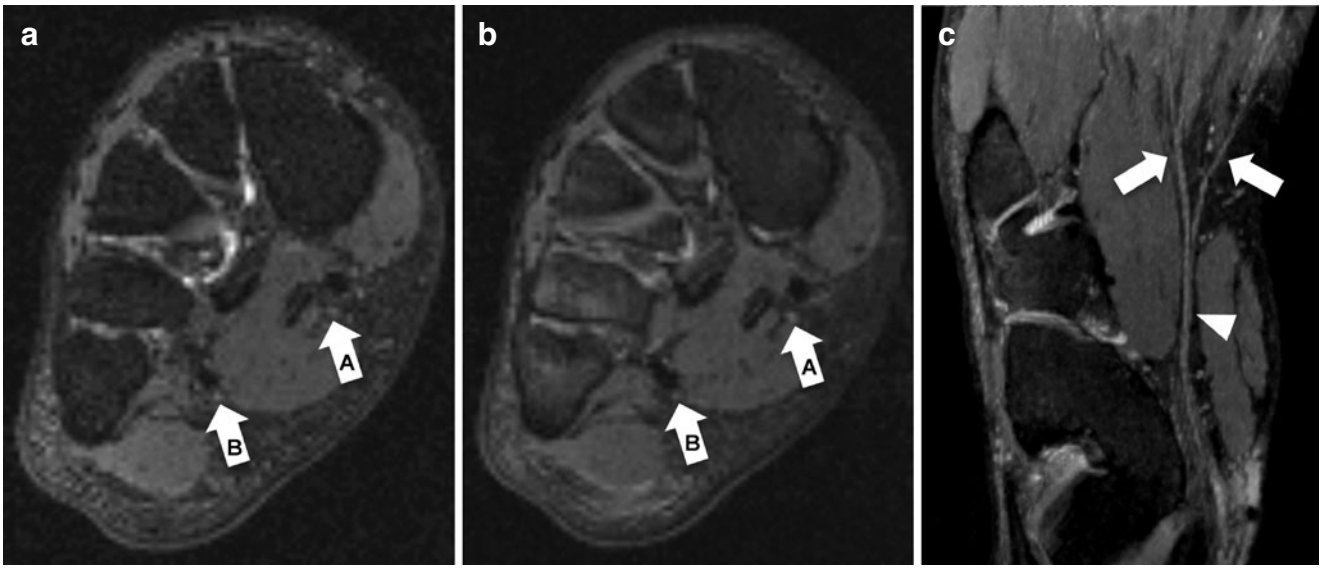

Fig. 1 Axial 3D DW-PSIF images of the midfoot (**a**, **b**) with varying diffusion moment values. An image with *b* value of 20 s mm^{-2} s^{-1} (**a**) shows incomplete suppression of the small vessels adjacent to the medial (*arrow* in **a**) and lateral (*arrow* in **b**) plantar nerves, whereas increasing the *b* value to 90 s $mm^{-2}s^{-1}$ (**b**) leads to excellent suppression of vessels creating nerve selective images. Isotropic coronal reformation (**c**) from the same image in **b** shows the medial plantar nerve (*arrowhead*) and its branches (*arrows*). Notice punctate scattered hyperintensities from fluctuating T2 SI of tiny vessels in the foot

nerves in the reconstructed axial plane, the images can be reformatted in any arbitrary plane (curved-planar reformation, CPR) without a significant loss of resolution. In addition, maximum intensity projections (MIP) may be used to further enhance the conspicuity of the nerves and produce longitudinal images, which can nicely depict the nerve anatomy and pathology (Fig. 3). This imaging evaluation can be easily accomplished on a workstation with capability of CPR and multiplanar reconstruction (MPR). The reconstructed slab thickness may be varied depending upon the size of the nerve, anywhere from 3 to 15 mm.

Anatomic depiction

It should be noted that 3D DW-PSIF does not replace conventional two-dimensional imaging. Initial imaging evaluation should be accomplished on conventional axial T1-weighted and fat-suppressed T2-weighted (FST2W) images due to the overall better soft tissue contrast and SNR on these sequences. It is our experience that the fascicular morphology of the nerves is also better depicted on conventional sequences than on the 3D DW-PSIF sequence (Fig. 4a, b). Reconstructed axial images from 3D DW-PSIF serve as problem-solving

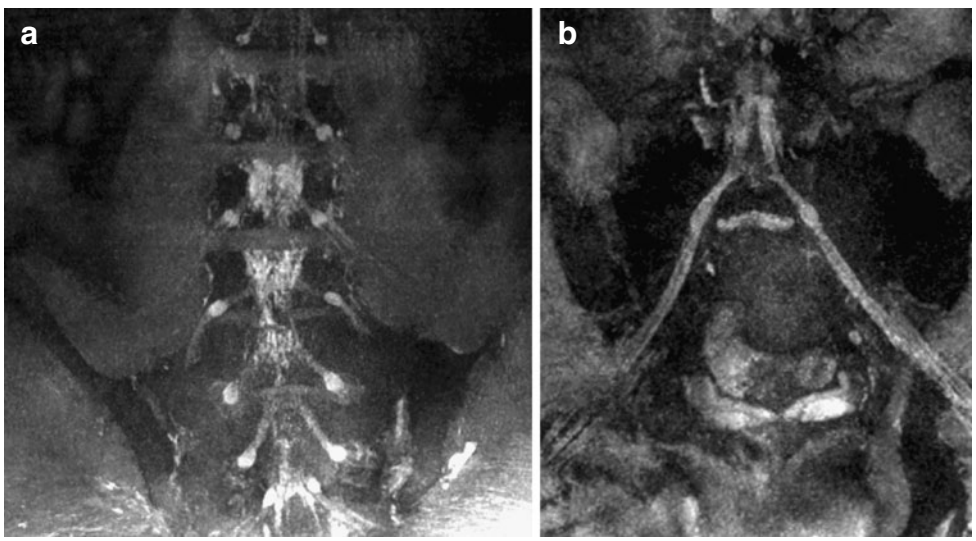

Fig. 2 Coronal 3D DW-PSIF images of the normal dorsal nerve root ganglia in lumbosacral plexus (**a**) and pelvic course of the sciatic nerves (**b**)

Table 1 The acquisition parameters employed for the 3D DW-PSIF sequence in the MR neurography examinations of the study

Acquisition parameter	Value
Slabs	1
Matrix size	120–420×100–120
Field of view	100–320×100 mm
Slice thickness	0.9 mm
TR	10 ms
TE	2.47 ms
Averages	1
Coil	4-channel or 8-channel surface coil
Flip angle	35°
Fat suppression	Water excitation normal
Diffusion mode	Phase
Diffusion directions	1
Dimension	3D
3D partitions	290
Effective spatial resolution	0.7–0.8×0.7–0.8×0.7–0.8 mm
b Value	80–90 s mm^{-2} s^{-1}
Elliptical scanning	On
Asymmetric echo	Off
Receiver bandwidth	439 Hz/Px
Acquisitions	1
Time of acquisition	4 min 28 s to 6 min 25 s

sequence to differentiate nerves from suppressed vessels (Fig. 4c). Normal nerves show intermediate signal intensity on 3D DW-PSIF imaging, while vessels lose their signal and become hypointense. Magic angle artifacts leading to increase in nerve signal [8] may occur on 3D DW-PSIF but seem to be less of a problem on these images than conventional imaging sequences. Following axial evaluation, MPR and CPR are performed. These nerve-specific images enable accurate confirmation of anatomic continuity of the nerve (important from the surgical perspective), depict their normal course as well as help in identification of secondary and tertiary branching (Fig. 1c, 3). 3D DW-PSIF is more efficient than the conventional T2-based sequences at differentiating small peripheral nerves from adjacent vessels, however, in vessels with a diameter of less than 3–5 mm, there may be incomplete suppression of flow signal. In the authors' experience, these vessels show fluctuating low and high signal intensity as opposed to the uniform intermediate signal intensity of the normal nerve, enabling easy differentiation (Fig. 1c). In the distal extremities, particularly distal to the knee and elbow joints, commonly encountered T2 hyperintense subcutaneous and/or fascial edema makes the identification of small peripheral nerves challenging on conventional T2-weighted sequences. In contrast, the inherent diffusion sensitive gradients of 3D DW-PSIF enable selective suppression of the water signal of the subcutaneous and fascial edema, thus improving the conspicuity of small peripheral nerves in the above areas (Fig. 5).

Fig. 3 MIP reconstruction of the normal sciatic nerve (*black arrow*) in the thigh with its tibial (*white arrow*) and common peroneal (*white arrowhead*) branches

Pathology depiction

3D DW-PSIF inherently provides predominantly T2 type of contrast and therefore depicts the nerve pathology as abnormal T2 hyperintensity similar to the conventional FST2W images. However, the signal abnormality on FST2W images may involve a very long segment of the nerve based on mechanisms of proximal axoplasmic flow and venous congestion and distal Wallerian degeneration [2, 9, 10]. Fascicular enlargement is similarly depicted on both sequences, however it is better appreciated on FST2W images due to inherently higher SNR and soft tissue contrast (Fig. 6a). The main advantage of 3D DW-PSIF is the easy generation of isotropic images using CPR and MPR for excellent depiction of the normal and abnormal (focally enlarged/decreased caliber) segments along the long axis of the nerve (Fig. 6b). Neuroma in continuity and nerve discontinuity (potential surgical lesions) are adequately differentiated from milder degrees of stretch/ischemic injuries (medical lesions), which only produce mildly abnormal T2 signal intensity or mildly abnormal fascicular changes. Focal nerve entrapments as well as focal or diffuse course deviations of nerve due to space-occupying lesions, such as focal fibrosis/tumors, are also adequately demonstrated (Fig. 7). MIP reconstructions produce excellent images that can be distributed to

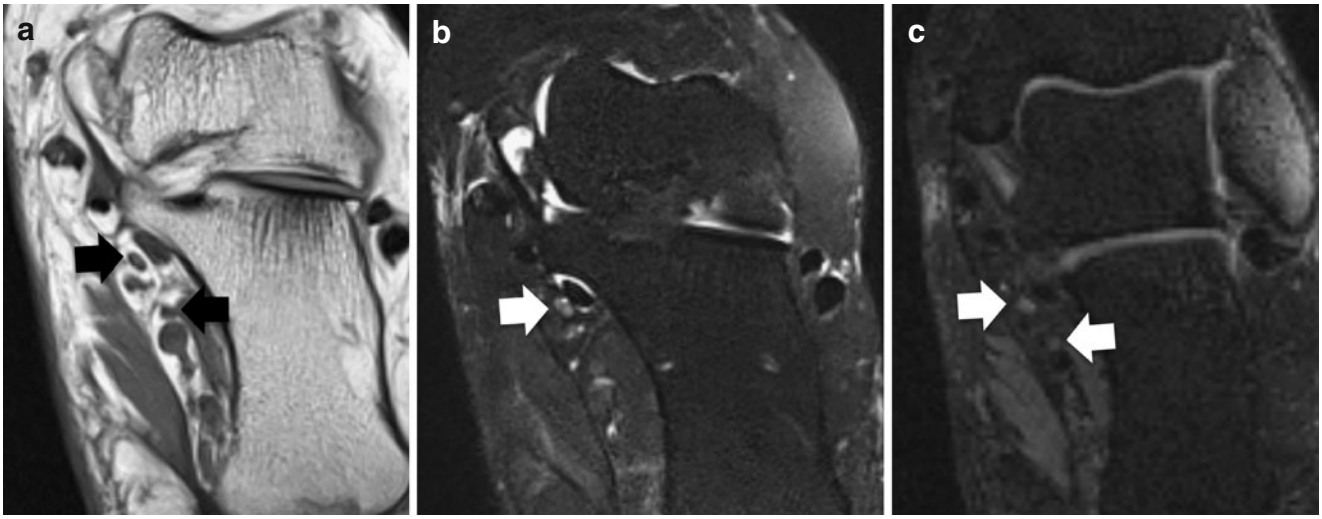

Fig. 4 **a**–**c** A 43-year-old male with ankle pain and clinically suspected medial plantar neuritis. Oblique axial T1-weighted image (**a**) shows the medial and lateral plantar nerves in their respective tunnels (*arrows*). Oblique axial T2 SPAIR image (**b**) shows the medial plantar nerve abnormality as abnormal T2 hyperintensity (*arrow*). Lateral plantar nerve is not clearly discerned. Notice on similarly reconstructed 3D DW-PSIF image (**c**) both medial and lateral plantar nerves are easily differentiated (*arrows*). Although fascicular appearance is better seen on T2-weighted image, abnormal T2 hyperintensity of the medial plantar nerve is readily apparent

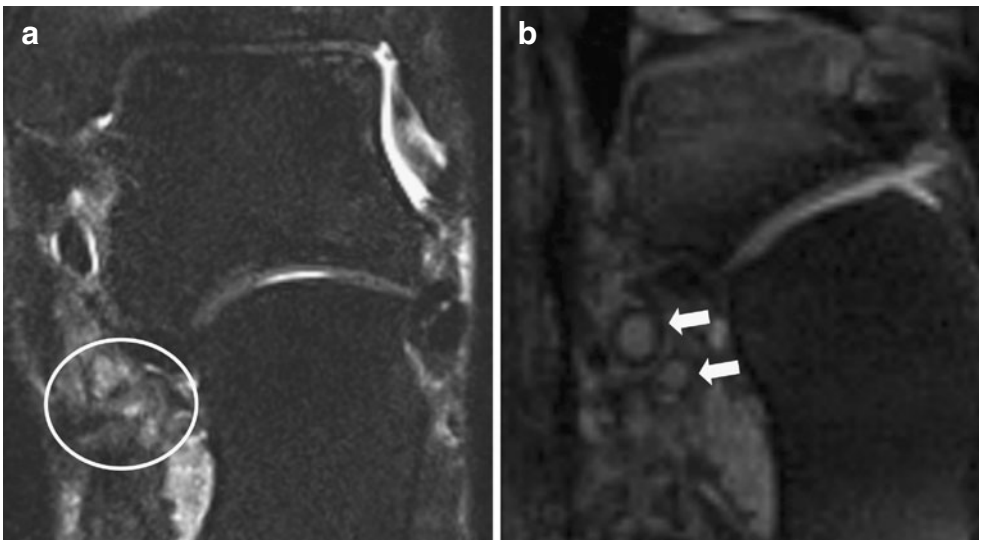

Fig. 5 **a**, **b** A 32-year-old female with medial and lateral plantar nerve entrapments following a repeat tarsal tunnel surgery. Due to surrounding post-operative changes and edema, the nerves are not easily seen on axial oblique T2 SPAIR image (*encircled* in **a**). Notice the depiction of the enlarged plantar nerves on the corresponding 3D DW-PSIF image (*arrows* in **b**)

the clinicians for better understanding and localization of the nerve pathology (Fig. 8). 3D DW-PSIF may also be used in post-contrast imaging similar to the 3D volumetric interpolated breath hold examination (3D VIBE) sequence in cases of suspected infection/inflammation or tumors for adequate assessment of the anatomic relationship between the nerves and enhancing intraneural and/or extraneural tumors [6]. Similar depiction of the lesions may be seen on both types of sequences (Fig. 9).

It should be noted that imaging with 3D DW-PSIF requires good shimming. The images may come out suboptimal, if off-center or larger areas (>15 cm craniocaudal coverage) are imaged. The fat saturation may fail in those circumstances and ghosting artifacts may degrade the images. In our experience, it performs best with joint-specific or good surface coils.

To conclude, 3D DW-PSIF sequence provides nerve-specific images and nicely depicts nerve anatomy and

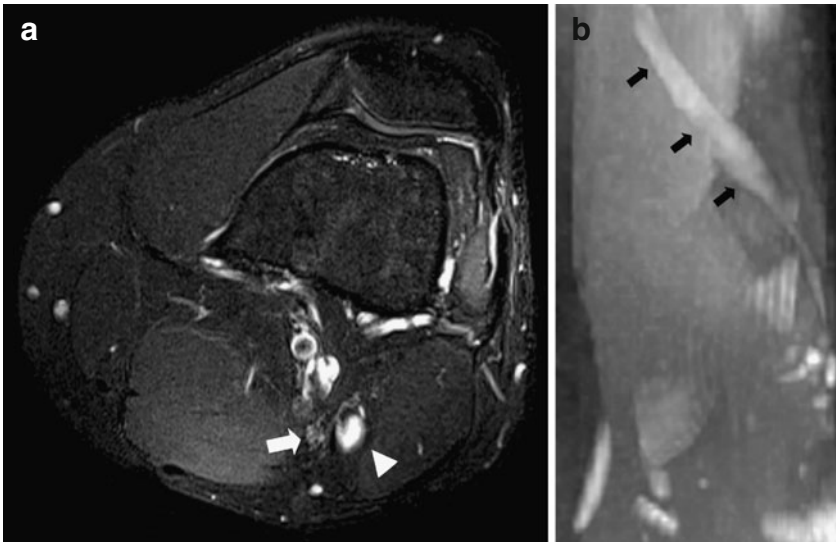

Fig. 6 **a**, **b** A 22-year-old male with previous knee injury. Notice mildly abnormal with hyperintense fascicles in the tibial nerve on axial T2 SPAIR image through the knee (*arrow* in **a**). The common peroneal nerve (CPN) is abnormally enlarged with fascicular disruption (*arrowhead* in **a**). MIP reconstruction of the CPN shows the full extent of the nerve pathology as a large neuroma in continuity, in keeping with high grade injury (*arrows* in **b**)

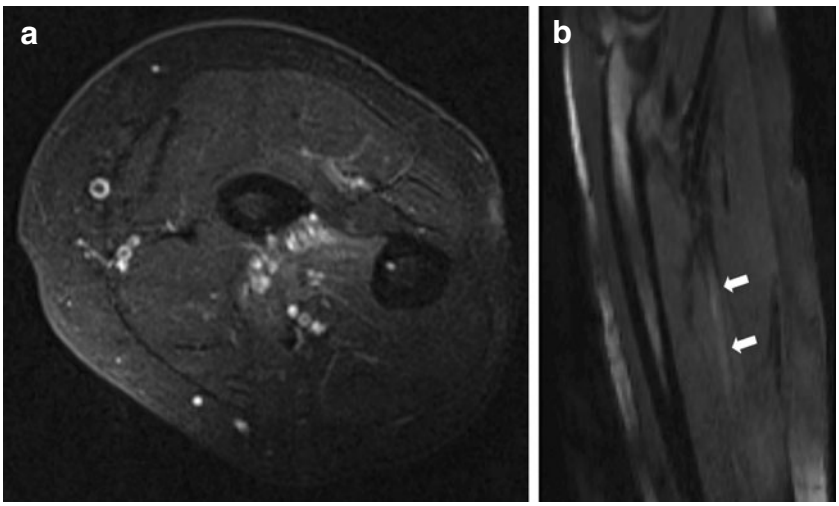

Fig. 7 **a**, **b** Median nerve entrapment in the proximal forearm. A 50-year-old female with symptoms of median nerve entrapment in the hand and negative electrodiagnostic findings of carpal tunnel syndrome was imaged in the forearm area. Axial T2 SPAIR image (**a**) shows denervation changes in the flexor compartment. The abnormal nerve is difficult to differentiate from the similarly intense vessels. On a 3D DW-PSIF reconstructed sagittal image (**b**), the median nerve (*arrows*) is focally enlarged and hyperintense, as well as entrapped at the flexor digitorum superficialis sheath

Fig. 8 A 13-year-old boy with biopsy-proven perineuroma of the common peroneal nerve. MIP reconstructed 3D DW-PSIF image through the leg shows the full extent of the perineuroma for presurgical mapping (*arrow*)

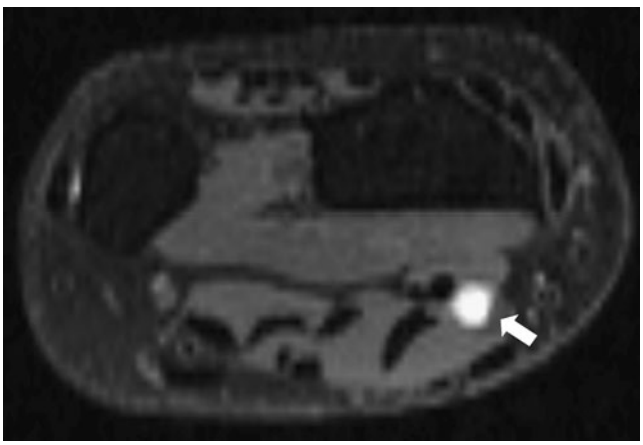

Fig. 9 A 37-year-old female with known median nerve schwannomatosis. Notice similar enhancement of the median nerve (*arrows*) on post-intravenous gadolinium 3D DW-PSIF (**a**) as well as T1 VIBE (**b**) images. Also, notice suppression of the contrast signal within the ulnar and median arteries on the 3D DW-PSIF images

pathology. This novel imaging sequence may be incorporated in the MR neurography examination protocol for accurate nerve localization and nerve pathology evaluation.

References

1. Andreisek G, Burg D, Studer A, Weishaupt D, et al. Upper extremity peripheral neuropathies: role and impact of MR imaging on patient management. Eur Radiol. 2008;18:1953–61.
2. Filler AG, Maravilla KR, Tsuruda JS. MR neurography and muscle MR imaging for image diagnosis of disorders affecting the peripheral nerves and musculature. Neurol Clin. 2004;22:643–82.
3. Chhabra A, Williams EH, Wang KC, Dellon AL, Carrino JA. MR neurography of neuromas related to nerve injury and entrapment with surgical correlation. AJNR Am J Neuroradiol. 2010;31:1363–8.
4. Zhang Z, Song L, Meng Q, Li Z, Pan B, Yang Z, et al. Morphological analysis in patients with sciatica: a magnetic resonance imaging study using three-dimensional high-resolution diffusion-weighted magnetic resonance neurography techniques. Spine (Phila Pa 1976). 2009;34:E245–50.
5. Stoller DW. Entrapment neuropathies of the lower extremity. In: Magnetic resonance imaging in orthopaedics and sports medicine. 3rd edition. Baltimore: Lippincott Williams & Wilkins; 2007. p. 1051–98
6. Zhang Z, Meng Q, Chen Y, et al. 3-T imaging of the cranial nerves using three-dimensional reversed FISP with diffusion-weighted MR sequence. J Magn Reson Imaging. 2008;27:454–8.
7. Zhang ZW, Song LJ, Meng QF, et al. High-resolution diffusion-weighted MR imaging of the human lumbosacral plexus and its branches based on a steady-state free precession imaging technique at 3 T. AJNR Am J Neuroradiol. 2008;29:1092–4.
8. Bowen BC. Peripheral nerve imaging and the magic angle. AJNR Am J Neuroradiol. 2004;25:352–4.
9. Baur A, Reiser MF. Diffusion-weighted imaging of the musculoskeletal system in humans. Skeletal Radiol. 2000;29:555–62.
10. Filler AG, Kliot M, Howe FA, et al. Application of magnetic resonance neurography in the evaluation of patients with peripheral nerve pathology. J Neurosurg. 1996;85:299–309.